JOURNAL OF COMPUTATIONAL PHYSICS 118, 222–228 (1995)

On the Numerical Treatment of Corner Singularity in the Vorticity Field

J. M. FLORYAN* AND L. CZECHOWSKI†

Department of Mechanical Engineering, The University of Western Ontario, London, Ontario, Canada, N6A 5B9

Received July 1, 1993; revised August 29, 1994

The error in simulation of viscous flows in domains with sharp corners has been evaluated for a model problem at zero Reynolds number. Methods based on a local analytical solution give reliable results but their applicability is limited. The ad hoc numerical methods give an error that is not negligible and has a nonlocal character in some parts of the flow. © 1995 Academic Press, Inc.

I. INTRODUCTION

Flows with either discontinuous boundary conditions or with an abrupt change in the boundary shape are of interest in many applications. Singularities induced by these effects may give rise to an additional error in the numerical solution of the field equations. Analysis of this error is the objective of this paper.

In order to simplify our presentation, we shall limit this discussion to the classical case of a viscous flow over a cavity (see Fig. 1). Several methods [10] have been proposed in order to approximate the singular behaviour of vorticity at the upper (convex) corners. While each of these methods produces a solution, it is not known which one is best and whether any of them provide an accurate approximation of the actual solution. Because of lack of anything better, these methods are widely used, with an implicit assumption being made that the error caused by the potentially improper treatment of singularity has at most a local character.

The purposes of this paper are (i) to estimate the error caused by different numerical treatments of the corner singularity and (ii) to verify the assumption regarding the local nature of such an error.

The first group of methods considered here combines a local analytical description of singularity (taken from Ref. [8]), which is valid in a small neighbourhood of the corner, with a purely numerical solution away from the corner. The idea of such mixing of numerical and analytical solutions was originally proposed by Motz [7]. We shall use grid convergence studies in order to test these methods.

The analytical solution [8] is valid in the case of zero Reynolds number flows. The nonzero Reynolds number flows have been purposely omitted from our tests in order to avoid additional uncertainties associated with the applicability of the analytical solution when convective terms are present.

The second group of methods uses ad hoc numerical approximations which do not require any particular knowledge of the structure of singularity. We have tested eight of them. Since it has been shown that the flow does not separate at the corner [11, 13], we have rejected any method based on this assumption [see Ref. 10]. We assess the accuracy of these methods by carrying out grid convergence studies and comparing the results with those obtained using methods based on the local analytical description of singularity.

In Section II we describe our test problem and its numerical solution. The analytical structure of singularity is reviewed in Section III. Numerical solutions incorporating an analytical description of singularity and proofs of their convergence are described in Section IV. A purely numerical treatment of singularity and the resulting error are discussed in Section V. An example where an algorithm based on an analytical description of singularity fails is given Section VI. A short summary of the main conclusions is given in Section VII.

II. PROBLEM FORMULATION

We consider flow over a cavity as sketched in Fig. 1. The appropriate field equations are the Navier–Stokes equations and the equation of continuity. The streamfunction–vorticity formulation is used which, in the Stokes limit, has the form

$$\nabla^2\psi = -\omega, \tag{1}$$

$$\nabla^2\omega = 0. \tag{2}$$

In the above, ψ denotes the streamfunction and ω stands for the vorticity. The appropriate boundary conditions are the conditions of no-slip and no-penetration at the solid boundaries. The inflow and outflow conditions correspond to a linear velocity distribution, as shown in Fig. 1.

* Professor.

† Visiting Fellow.

0021-9991/95 $6.00

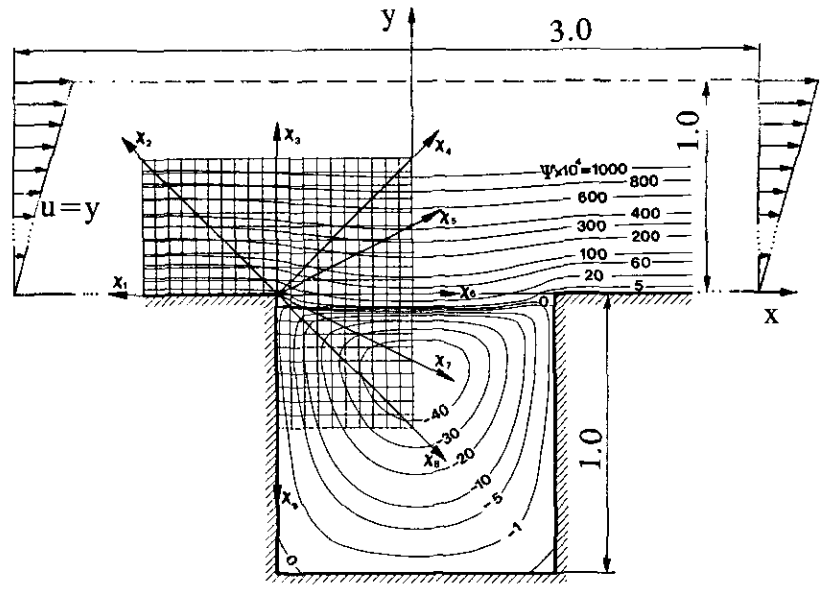

FIG. 1. Sketch of the flow domain. The results are based on method A (see text). The error distribution along line x_8 due to approximate treatment of singularity is shown in Fig. 4.

$$\psi = \frac{\partial \psi}{\partial y} = 0 \qquad \text{at } y = 0 \text{ for } \tfrac{1}{2} \leq |x| \leq \tfrac{3}{2}, \tag{3a}$$

$$\psi = \frac{\partial \psi}{\partial y} = 0 \qquad \text{at } y = -1 \text{ for } |x| \leq \tfrac{1}{2}, \tag{3b}$$

$$\psi = \frac{\partial \psi}{\partial x} = 0 \qquad \text{at } x = \pm \tfrac{1}{2}, -1 \leq y \leq 0, \tag{3c}$$

$$\psi = y^2/2, \omega = -1 \qquad \text{at } x = \pm \tfrac{3}{2}, 0 \leq y \leq 1, \tag{3d}$$

$$\psi = \tfrac{1}{2}, \omega = -1 \qquad \text{at } y = 1, -3/2 \leq x \leq 3/2. \tag{3e}$$

A square computation grid of size Δ is used, with grid lines parallel to the x and y and such that the grid fits exactly the geometry of the channel, with the walls as certain grid lines. Around a typical internal grid point (x_0, y_0), we adopt the convention that the quantities at (x_0, y_0), $(x_0 + \Delta, y_0)$, $(x_0, y_0 + \Delta)$, $(x_0 - \Delta, y_0)$, and $(x_0, y_0 - \Delta)$ are denoted by subscripts 0, 1, 2, 3, and 4 respectively. The (1) and (2) are then approximated by using central differences at (x_0, y_0) in the usual manner, to give

$$\psi_1 + \psi_2 + \psi_3 + \psi_4 - 4\psi_0 + \Delta^2 \omega_0 = 0, \tag{4}$$

$$\omega_1 + \omega_2 + \omega_3 + \omega_4 - 4\omega_0 = 0. \tag{5}$$

The boundary conditions for the Eqs. (4)–(5) are given by (3). The values of ω required at grid points on the solid walls are evaluated using a second-order approximation [9]

$$\omega_b = \frac{1}{2\Delta^2}(\psi_{j+1} - 8\psi_j + 7\psi_b). \tag{6}$$

In the above, the subscript b refers to a value at the appropriate boundary point, the subscript j refers to the internal grid point most immediate to b, and the subscript $j + 1$ corresponds to the next interior grid point in the same direction.

All the equations were solved by a successive underrelaxation procedure. The iterations were performed until the convergence criteria $|\omega_0^{k+1} - \omega_0^k| < 10^{-9}$ and $|\psi_0^{k+1} - \psi_0^k| < 10^{-9}$, with k denoting the iteration number, were satisfied at all grid points.

III. CORNER SINGULARITY

With the grid structure used the (upper) corner points $(x = \pm\frac{1}{2}, y = 0)$, where the vorticity is singular, are the grid points. This renders the finite difference approximation (5) invalid at the grid points $(x_0, y_0) = (-\frac{1}{2}, \Delta)$, $(x_0, y_0) = (-\frac{1}{2} + \Delta, 0)$, $(x_0, y_0) = (\frac{1}{2} - \Delta, 0)$ and $(x_0, y_0) = (\frac{1}{2}, \Delta)$. One may note that while the bottom corners are also grid points, they do not enter the calculations and the vorticity is not singular there.

It can be shown [11] that near an external corner, the streamfunction and vorticity can be described in terms of infinite series, whose two leading order terms have the form:

$$\begin{aligned}\psi(r, \theta) = {} & A_1 r^{\lambda_1} \{\cos[3\pi(\lambda_1 - 2)/4] \cos(\lambda_1 \theta) \\ & - \cos(3\pi\lambda_1/4) \cos[(\lambda_1 - 2)\theta]\} \\ & + A_2 r^{\lambda_2} \{\sin[3\pi(\lambda_2 - 2)/4] \sin(\lambda_2 \theta) \\ & - \sin(3\pi\lambda_2/4) \sin[(\lambda_2 - 2)\theta]\} + \ldots \end{aligned} \tag{7a}$$

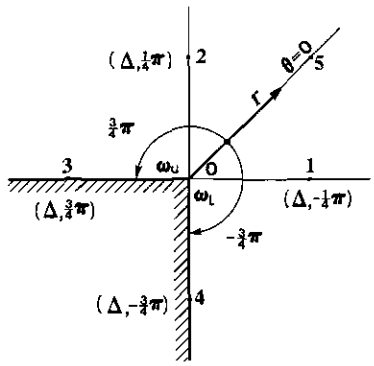

FIG. 2. Grid points around an external corner.

$$\omega(r, \theta) = 4A_1 r^{\lambda_1 - 2}(\lambda_1 - 1)\cos(3\pi\lambda_1/4)\cos[(\lambda_1 - 2)\theta] + 4A_2 r^{\lambda_2 - 2}(\lambda_2 - 1)\sin(3\pi\lambda_2/4)\sin[(\lambda_2 - 2)\theta] + \ldots. \quad (7b)$$

In the above, r is the radial distance from the corner and the angle θ is as defined in Fig. 2 with $\theta = 0$ bisecting the corner angle, $\lambda_1 = 1.5444837$ and $\lambda_2 = 1.9085292$. The constants A_1 and A_2 corresponding to the antisymmetric and symmetric parts of the flow around $\theta = 0$, respectively, have to be determined from flow conditions away from the corner.

IV. NUMERICAL SOLUTION WITH ANALYTICAL DESCRIPTION OF THE SINGULARITY

Application of Eq. (7) is explained with the help of Fig. 2. The ω_0 value is singular and it renders the finite difference approximation (5) invalid at points 1 and 2. The ω_1 and ω_2 are, therefore, evaluated from (7b) converting points 1 and 2 into boundary points for the vorticity field. Constants A_1 and A_2 are evaluated by matching (7) with the numerical solution. Various matching methods can be summarized as follows:

Method A: Determine A_1 and A_2 from the known vorticity at points 3 and 4 (the values of ω_3 and ω_4 have to be updated sequentially during the iteration process).

Method B: Determine A_1 and A_2 from the known values of streamfunction at points 1 and 2 (the values ψ_1 and ψ_2 have to be updated sequentially during the iteration process).

Method C: Use method A but also impose values of ψ at 1 and 2 from Eq. (7a) rather than from Eq. (4).

Method D: Use method B but also impose values of ω at 3 and 4 from Eq. (7b) rather than from Eq. (6).

Method E: Use the formula

$$\omega_0 = -1.75042\,\frac{\psi_2 + \psi_1}{\Delta^2}.$$

Method A has been used by Bramley and Dennis [1] and Shen and Floryan [11]. Holstein and Paddon [3] incorporated (7) by introducing a fictitious (finite) value of vorticity at the corner. This value is obtained by taking only the first term on the right hand side of (7a) and determining A_1 through matching with the symmetric (around $\theta = 0$) part of the streamfunction (as represented by ψ_1 and ψ_2). This leads to Method E which should properly account for the magnitude of vorticity, but which may not be able to reproduce accurately certain topological features of the flow field around the corner like, for example, location of the separation point. Shen *et al.* [11] used (7) to construct a special element for analysis of creeping flows around sharp corners using finite element discretization. Ladeveze and Peyret [5] incorporated (7) into a finite difference algorithm in a primitive variables formulation.

Success of all of the above methods hinges on the applicability of Eqs. (7), which is only valid in the asymptotic limit of $r \to 0$ (i.e., in a sufficiently small neighbourhood of the corner). Since the matching always takes place at a finite distance away from the corner, the question arises whether use of (7) can be justified. In the absence of exact solution, this issue will be tested by grid convergence studies. We note that if (7) provides an accurate approximation of the solution at a distance Δ away from the corner, then all of the above methods should produce identical (within the error of approximation) results.

Tables Ia–Ie give constants A_1 and A_2 computed on the basis of methods A–E. Results show that while the computed values do converge as a function of Δ, they appear to approach different

TABLE Ia

Constants A_1 and A_2 Computed on the Basis of Method A

Δ	$A_1(\omega_3, \omega_4)$	$A_2(\omega_3, \omega_4)$	$A_1(\psi_1, \psi_2)$	$A_2(\psi_1, \psi_2)$
0.1	0.1807915	−0.7867092	0.1385074	−0.8399356
0.05	0.1633243	−0.7970514	0.1328204	−0.8366852
0.025	0.1548943	−0.8013786	0.1288704	−0.8365979
0.0125	0.1508968	−0.8030848	0.1264776	−0.8370210
0.00625	0.1490467	−0.8037241	0.1251384	−0.8373481

Note. Values of A_1 and A_2 computed from ψ_1 and ψ_2 are given for comparison purposes.

TABLE Ib

Constants A_1 and A_2 Computed on the Basis of Method B

Δ	$A_1(\psi_1, \psi_2)$	$A_2(\psi_1, \psi_2)$	$A_1(\omega_3, \omega_4)$	$A_2(\omega_3, \omega_4)$
0.1	0.1689749	−0.8224835	0.2265245	−0.7741082
0.05	0.1555963	−0.8247175	0.1974867	−0.7884542
0.025	0.1485831	−0.8264075	0.1844199	−0.7941451
0.0125	0.1450987	−0.8274104	0.1787600	−0.7963145
0.00625	0.1432484	−0.8279951	0.1761787	−0.7971947

Note. Values of A_1 and A_2 computed from ω_3 and ω_4 are given for comparison purposes.

TABLE Ic

Constants A_1 and A_2 Computed on the Basis of Method C

Δ	A_1	A_2
0.1	0.2024630	−0.7733487
0.05	0.1755533	−0.7857563
0.025	0.1641912	−0.7901927
0.0125	0.1591173	−0.7917119
0.00625	0.1570712	−0.7923180

TABLE Ie

Constant A_1 Computed on the Basis of Method E

Δ	A_1 (ψ_1, ψ_2)	A_2 (ψ_1, ψ_2)	A_1 (ω_3, ω_4)	A_2 (ω_3, ω_4)
0.1	0.1395129	−0.9338717	0.1821792	−0.8522522
0.05	0.1356366	−0.9333481	0.1675329	−0.8645927
0.025	0.1338410	−0.9333427	0.1623412	−0.8690145
0.0125	0.1330480	−0.9334358	0.1607021	−0.8705054
0.00625	0.1326736	−0.9335018	0.1603158	−0.8709720

Note. Values of A_2 (not used in the solution of the field equations) computed from ψ_1 and ψ_2, and A_1 and A_2 computed from ω_3 and ω_4 are given for comparison purposes.

limits depending on the method used. Methods A and B demonstrate that the basic assumption underlying the algorithm, i.e., that we are sufficiently close to the corner to be able to use (7), is not fulfilled even for $\Delta = 0.00625$.

Analysis of results of grid convergence studies shows that A_1 converges at a rate very close to the theoretical one of $\Delta^{1.08}$, with the methods based on matching of streamfunction having the exponent smaller by 10–15%. A_2 converges at a rate close to the theoretical one of $\Delta^{1.39}$ for methods A and C, with the exponent reduced by about 50% for methods B and D. Theoretical values have been obtained by noting that the dominant symmetric term in the truncated part of (7a) is $0(r^{2.62})$ and the dominant antisymmetric term is $0(r^{3.3})$ (see, for example, Ref. (3)).

It may be concluded on the basis of the above results that the structure of the numerical solution is correct and accurate results can be obtained by further reduction of the grid size.

Since methods A–E are based on different implementations of (7), they are not computationally equivalent and one should not be surprised by the fact that they produce slightly different results (see Tables Ia–Ie). If the principle underlying the algorithm is correct, however, these differences should have only a local character and should decrease with distance away from the corner. Figure 3a shows the results of testing of methods A and E with the matching points moved by distance 4Δ away from the corner (A_1 and A_2 are calculated from vorticity at points M and N of Fig. 3a). High grid density was obtained using local grid refinement around the corner. These results show that A_1 and A_2 tend to values independent of Δ and independent of the method used to implement (7). As a second test, A_1 and A_2 were calculated using values of vorticity at nine

TABLE Id

Constants A_1 and A_2 Computed on the Basis of Method D

Δ	A_1	A_2
0.1	0.1711653	−0.8169246
0.05	0.1572662	−0.8207434
0.025	0.1500948	−0.8228899
0.0125	0.1464405	−0.8239667
0.00625	0.1446062	−0.8247189

pairs of points located symmetrically with respect to the corner (Fig. 3a). Figure 3b shows that the square mean deviation σ of A_1 and A_2 from the mean value decreases with a decrease of Δ. Here, σ is defined as $\sigma = \frac{1}{8}\sqrt{\Sigma_{n=1}^{9}(A_{nk} - A_{mk})^2}$, where $A_{mk} = \frac{1}{9}\Sigma_{n=1}^{9} A_{nk}$ and $k = 1(2)$ corresponds to A_1 (A_2).

The above tests confirm convergence of methods based on local analytical description of singularity for this test problem. This convergence is not generally guaranteed and, as a matter of fact, Section VI describes a test problem where such methods fail.

The convergence of methods discussed in this Section is of obvious advantage. Present results indicate that good approximation is obtained only for very fine grids, e.g., $\Delta < \frac{1}{512}$. This means that for larger Δ the truncated expansion (7) is not sufficiently accurate. Several tests were made with two more terms from the complete expansion [8] added to (7). Since the exponents λ now become complex, six real constants had to be determined from matching with the numerical solution. Because it was not possible to demonstrate convergence of the additional constants as a function of Δ, this approach was not pursued.One should note that complex exponents λ correspond to solutions that are oscillatory in r and therefore may have no physical meaning in the problem studied. Because of the inconclusive results of the numerical experiments, we cannot make convincing arguments either against or for retention of these terms.

One may argue, on the basis of results presented above, that in spite of sound theoretical basis, the methods described in this section are impractical due to excessive requirements on grid size. It will be shown in the next section that, nevertheless, there is no alternative if accuracy is important.

V. PURELY NUMERICAL SOLUTIONS

The ad hoc numerical methods for resolving the singularity problem used in the present study are as follows:

Method F: Two discontinuous wall values of ω are assigned

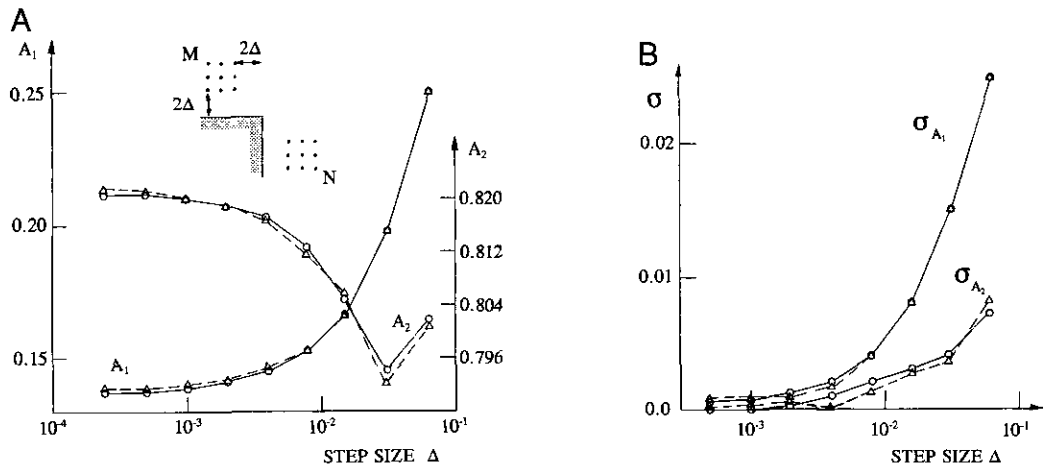

FIG. 3. Results of the convergence tests for methods A (—) and E (---). (A): constants A_1 and A_2 evaluated from vorticity at points M and N. (B): mean deviation σ of constants A_1 and A_2 evaluated from vorticity at pairs of points located symmetrically with respect to the corner (see (A) for location of these points).

to point 0 in Fig. 2. The upstream value ω_u is evaluated by applying (6) along the vertical grid line, and the downstream value ω_l is obtained by applying (6) along the horizontal grid line [10].

Method G: The average of wall values of ω is used at point 0 in Fig. 2 [10], i.e.,

$$\omega_0 = \tfrac{1}{2}(\omega_l + \omega_u).$$

Method H: Only the upstream value of ω is used at point 0 in Fig. 2 [10], i.e.,

$$\omega_0 = \omega_u.$$

Method I: Symmetry of ψ around 0 is assumed ($\psi_3^* = \psi_1$, $\psi_4^* = \psi_2$ in Fig. 2, Kawaguti method [10]), i.e.,

$$\omega_0 = -2(\psi_1 + \psi_2)/\Delta^2.$$

Method J: The corner is cut by drawing a straight line between 3 and 4 in Fig. 2, i.e.,

$$\omega_0 = (-\psi_1 - \psi_2 + 4\psi_0)/\Delta^2.$$

Method K: The finite-difference approximation at 1 and 2 is applied along lines inclined at 45° to the main grid lines, thus avoiding use of the value of ω at the corner (see [2, 10]).

Method L: Symmetry of ψ around $\theta = 0$ in Fig. 2 is assumed, i.e.,

$$\omega_0 = -(\psi_1 + \psi_2)/\Delta^2.$$

Method M: Corner is assumed to be inclined at 45° to the

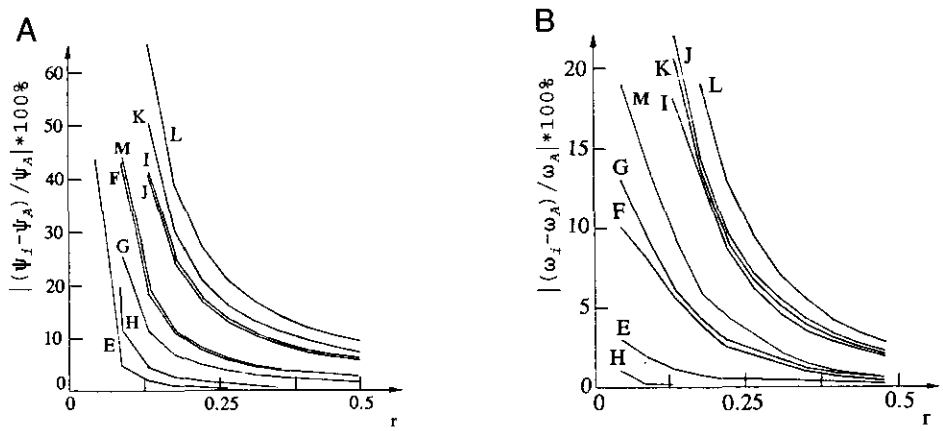

FIG. 4. Distribution of the relative error of the streamfunction (A) and vorticity (B) along line x_8 (see Fig. 1). The lines labelled E–M denote the error resulting from methods E–M, respectively, for $\Delta = \frac{1}{32}$.

TABLE IIa

Maximum Value of the Relative Error of Vorticity Determined on the Basis of Methods E–M

	Δ			
Method	$\frac{1}{16}$	$\frac{1}{32}$	$\frac{1}{64}$	$\frac{1}{128}$
E	0.8	0.4	0.2	0.1
F	3.5	1.9	1.0	0.4
G	4.4	2.2	1.1	0.4
H	0.9	0.1	0.2	0.4
I	13.5	6.2	2.8	1.3
J	15.7	7.3	3.4	1.7
K	12.8	6.9	3.5	2.0
L	19.3	9.5	4.5	2.9
M	6.2	3.1	1.5	0.8

Note. See text for details.

horizontal axis and vorticity is evaluated using one-sided finite-difference approximation along diagonal line ($\theta = 0$) in Fig. 5 (method 4 from [10]), i.e.,

$$\omega_0 = -\psi_5/\Delta^2$$

where ψ_5 denotes value of ψ at point 5 in Fig. 2.

To examine the accuracy of the above methods, we calculated the relative errors defined as $|(\psi_i - \psi_A)/\psi_A| * 100\%$ and $|(\omega_i - \omega_A)/\omega_A| * 100\%$ along nine directions shown in Fig. 1. Here, the subscript A denotes results obtained with method A (our reference method) and subscript i indicates one of the remaining methods (F–M). We have also included method E in these comparisons. The distributions of errors along direction x_8 are displayed in Fig. 4. Their maximum values found within the limit $\frac{1}{4} \le r \le \frac{1}{2}$, which can be used as a simple measure of their nonlocality, are given in Tables IIa and IIb.

TABLE IIb

Maximum Value of the Relative Error of Streamfunction Determined on the Basis of Methods E–M

	Δ			
Method	$\frac{1}{16}$	$\frac{1}{32}$	$\frac{1}{64}$	$\frac{1}{128}$
E	3.1	0.4	0.2	0.1
F	13.7	5.8	2.8	0.7
G	6.6	3.7	2.2	0.7
H	7.7	1.4	0.1	0.2
I	30.6	13.3	5.9	2.8
J	25.3	12.9	6.5	3.4
K	33.4	16.1	8.1	5.5
L	46.0	20.9	9.6	4.7
M	11.1	5.9	3.0	1.6

Note. See text for details.

Methods A and E are based on different implementations of the local analytical solution but give similar results, as discussed in Section IV. In the neighborhood of the corner the discrepancy may be substantial but at a distance larger than several Δ it is negligible, Table 2, Figure 4. The success of method E, which forces the streamfunction to be symmetric around $\theta = 0$ in Fig. 2, led us to proposing method L, which directly uses the symmetry property in the finite-difference discretization.

The error in determination of the streamfunction using ad-hoc numerical methods (F–M) is largest in the neighbourhood of the corner, but decreases with increasing distance. Solution outside the cavity is affected little by the singularity treatment. Inside the cavity the relative error is substantial even around the centre of the cavity and this shows that the error cannot be treated as a local phenomenon only. Its largest values concentrate around the separation streamline and it is unlikely that the location of this streamline can be accurately determined using any ad hoc approximation. Qualitatively, all methods give a similar error distribution, with method H giving the smallest values. It is worth noting that method H is least affected by the flow separation phenomenon.

The qualitative distribution of the vorticity error is similar to the error in streamfunction, as can be seen in Fig. 4b. This error is nonlocal inside the cavity and its largest values occur along the cavity's side wall. Method H gives the smallest values while method I the largest ones.

We can summarize the above discussion by stating that the approximate numerical treatment of the corner singularity results in an error that has a non-local character. The error persists even at considerable distances away from the corner in the separated part of the flow. The numerical method that assigns corner values of vorticity which are least affected by the separation phenomenon gives the smallest error.

The actual selection of the best or easiest to use method is left to the reader and his willingness to accept a certain level of uncertainty in the results. Data given in this paper should help to estimate this uncertainty. For example, if one works

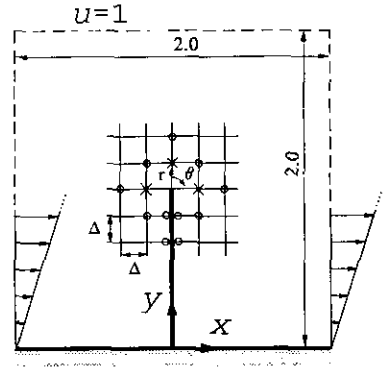

FIG. 5. Flow around an infinitely thin barrier. (+) denotes points for which discretization (5) is not valid. (○) denotes points of matching between numerical and analytical solutions.

TABLE III

Constants in Eq. (8) Determined from Matching with the Numerical Solution

Coeff.	Δ	0.1	0.05	0.025
$A_{-1/2}$		0.3239×10^{-10}	0.1925×10^{-10}	0.1136×10^{-10}
$B_{-1/2}$		0.2118	0.2276	0.2350
B_0		−4.992	−7.642	−11.26
$A_{1/2}$		0.2098×10^{-8}	0.3511×10^{-8}	0.5455×10^{-8}
$B_{1/2}$		12.4	26.83	56.31
A_1		-0.4986×10^{-7}	-0.1142×10^{-7}	-0.2536×10^{-7}
B_1		−21.67	−65.42	−195.5
$A_{3/2}$		0.9220×10^{-8}	0.2907×10^{-7}	0.9046×10^{-7}
$B_{3/2}$		23.83	102.4	436.6
A_2		-0.7960×10^{-8}	-0.3411×10^{-7}	-0.1467×10^{-6}
B_2		−13.62	−84.49	−513.0

with $\Delta = \frac{1}{16}$ and is prepared to accept 5% error for vorticity and 20% error for streamfunction, then all methods with exception of K give the same results.

VI. FAILURE OF METHOD BASED ON ANALYTICAL DESCRIPTION OF SINGULARITY

Results discussed in Section IV may leave one with an impression that an algorithm incorporating a local analytical description of singularity always produces accurate results (assuming that a sufficiently refined grid is used). As a counterexample, we consider a model problem involving Stokes flow around an infinitely thin barrier, as shown in Fig. 5. The structure of the solution around the tip has been given in the form of infinite series by Lugt and Schwidersky [6].

$$\begin{aligned}\omega(r,\theta) = {} & A_{-1/2}\, r^{-1/2} \sin(\theta/2) + B_{-1/2}\, r^{-1/2} \cos(\theta/2) \\ & + B_0 + A_{1/2}\, r^{1/2} \sin(\theta/2) \\ & + B_{1/2}\, r^{1/2} \cos(\theta/2) + A_1\, r \sin\theta \\ & + B_1\, r \cos\theta + A_{3/2}\, r^{3/2} \sin(3\,\theta/2) \\ & + B_{3/2}\, r^{3/2} \cos(3\,\theta/2) + A_2\, r^2 \sin(2\,\theta) \\ & + B_2\, r^2 \cos(2\,\theta) + \cdots .\end{aligned} \tag{8}$$

The notation is explained in Fig. 5. We have retained 11 terms in the expansion to make the truncation error smaller than the discretization error. The eleven constants were determined by matching numerical and analytical solutions for vorticity at eleven grid points shown in Fig. 5. Since the flow is symmetric with respect to the barrier, six constants in (8) should be zero. In the calculations, all 11 constants were retained and the symmetry condition was used to assess the accuracy of calculations. Results shown in Table III indicate that coefficients A_i and B_i do not converge with decreasing Δ. The same problem has been resolved using other sets of grid points for the matching purposes and with decreasing grid size of up to $\Delta = \frac{1}{128}$ without affecting the above conclusion.

VIII. CONCLUSIONS

A. The error due to a purely numerical treatment of singularity at the external corner in the vorticity field has been evaluated. The results indicate that the error is not negligible and has a nonlocal character in the separated part of the flow. The area around the separation streamline is affected the most.

B. Even when using a method that is well founded theoretically (i.e., a method based on a local analytical solution), one must be cautious. The advantage of the method may be evident only for a very fine grid. A possibility of failure of such a method has been demonstrated.

ACKNOWLEDGMENTS

This work has been supported by the NSERC of Canada and KBN of Poland.

REFERENCES

1. J. S. Bramley and S. C. R. Dennis, *Comput. Fluids* **12,** 339 (1984).
2. S. C. R. Dennis and F. T. Smith, *Proc. R. Soc. London, A* **372,** 393 (1980).
3. H. Holstein and D. J. Paddon, *J. Non-Newtonian Fluid Mech.* **8,** 81 (1981).
4. H. Holstein and D. J. Paddon, *Numerical Methods in Fluid Dynamics,* edited by K. W. Morton and M. J. Barnes (Academic Press, New York 1982), p. 341.
5. J. Ladeveze and R. Peyret, *J. Mecan.* **13,** 367 (1974).
6. H. J. Lugt and E. W. Schwiderski, *Proc. Roy. Soc. A.* **285,** 382 (1965).
7. M. Motz, *Q. Appl. Math.* **4,** 371 (1946).
8. H. K. Moffat, *J. Fluid Mech.* **18,** 1 (1964).
9. R. Peyret and T. D. Taylor, *Computational Methods for Fluid Flow,* (Springer-Verlag, New York/Berlin, 1983).
10. P. J. Roache, *Computational Fluid Dynamics,* Hermosa, Albuquerque, NM, 1976).
11. C. Shen and J. M. Floryan, *Phys. Fluids* **28,** 3191 (1985).
12. S. F. Shen, M. A. Morjaria, and R. K. Upadhyay, in *Proc. 1st. Int. Conf. on Numerical Methods in Laminar and Turbulent Flow, Swansea, U.K., 1978,* edited by C. Taylor *et al.,* (Pentech Press, London, 1978), p. 959.
13. S. Taneda, *J. Phys. Soc. Japan* **46,** 1935 (1979).